

Type of the Paper (Abstract, Meeting Report, Preface, Proceedings, etc.)

Influence of nonpolar medium on antioxidant capacity of bergaptol and xanthotoxol - kinetic DFT study[†]

Žiko Milanović^{1,*}, Marko Antonijević², Jelena Đorović Jovanović², Edina Avdović², Dejan Milenković², and Zoran Marković²

¹ University of Kragujevac, Faculty of Science, Department of Chemistry, Radoja Domanovića 12, 34000 Kragujevac, Serbia; e-mail: ziko.milanovic@pmf.kg.ac.rs

² University of Kragujevac, Institute for Information Technologies, Department of Science, Jovana Cvijića bb, 34000 Kragujevac, Serbia; e-mail: mantonijevic@uni.kg.ac.rs, j.djorovic@uni.kg.ac.rs, edina.avdovic@pmf.kg.ac.rs, deki82@kg.ac.rs, zmarkovic@uni.kg.ac.rs

* Correspondence: ziko.milanovic@pmf.kg.ac.rs; Tel.: +381-34-335-039

† Presented at the title, place, and date.

Received: date; Accepted: date; Published: date

Abstract: Within this study, the antioxidant capacity of bergaptol (BER) and xanthotoxol (XAN) in a nonpolar environment (benzene) was investigated against the reference standard Trolox (Tx). The ability to inactivate HO• radicals from the kinetic aspect was examined through hydrogen atom transfer (HAT), single-electron transfer–proton transfer (SET-PT), sequential proton loss electron transfer (SPLET), and radical adduct formation (RAF) mechanisms. The rate constants of the chemical reaction were calculated using the conventional transition state theory (TST) and Eckart method (ZCT₀). The research is based on a QM-ORSA (Quantum Mechanics–based test for Overall free-Radical Scavenging Activity) protocol. For this purpose, the *Gaussian 09* software package with the M06-2X/6-311++G(d,p) theoretical model was used. Both compounds in benzene have been shown to inactivate the HO• radical via HAT and RAF mechanisms. The calculated kinetic parameters indicate that the TST method, in some positions, is not suitable for calculating reaction rate constants at room temperature. Based on relative antioxidant capacity (r^T), both compounds showed better antioxidant capacity than Tx, while BER showed better activity than XAN. Based on the relative amount of products (Γ_i) of both compounds, it was concluded that the formation of a radical adduct in positions C-3, C-5, C-8, and C-2' is the most represented.

Keywords: Bergaptol; Xanthotoxol, QM-ORSA, DFT, Kinetic approach.

1. Introduction

Reactive oxygen species (ROS) are highly reactive and unstable radical species that are generated in the oxidative metabolism of aerobic cells. Because of unpaired electrons in the outer orbital, ROS very "aggressive" react with other biologically important components [1]. Formed as an intermediate product of oxygen metabolism by aerobic organisms, these species play an important role in cellular signaling (defence mechanism in the fight against various pathogens). On the other hand, overproduction of these species can lead to disturbances of fine balance and uncontrolled formation leading to oxidative stress [2,3].

The hydroxy radical (HO•) is a product of partial oxygen reduction and is a highly reactive species with an extremely short half-life (10^{-9} s). It is characterized by high electrophilicity and high thermochemical reactivity. As a strong oxidizing agent, the HO• reacts rapidly with organic and inorganic molecules in the cell, including DNA molecules (attacking purine and pyrimidine bases),

protein (amino acids), lipids, metals, and others constituents important for the integrity of cellular functionalities [4,5].

Furanocoumarins represent a large class of compounds present in the plant world (*Apiaceae*, *Rutaceae*, *Moraceae*, and *Fabaceae*), mostly in plants that have bloomed and in mature seeds and fruits. These compounds are characterized by numerous pharmacological properties [6]. A large number of furanocoumarin derivatives have been found to inhibit the formation and encourage the inactivation of reactive oxygen species [7]. Literature data show that the structural analogy with flavonoids and benzophenones is responsible for antioxidant activity, with the conclusion that the exact molecular mechanism of action has not been fully elucidated [8].

The aim of this study is to investigate the ability of two bioactive natural furanocoumarins: bergaptol (**BER**) and xanthoxol (**XAN**) in inactivating HO• radical (Figure 1) [9]. Available literature data indicate significant *in vitro* antioxidant abilities of **BER** ((2,2-azobis(3-ethylbenz-thiazoline-6-sulfonic acid) (ABTS) and 2,2-diphenyl-1-picrylhydrazil (DPPH) methods) and **XAN** (effective in preventing lipid peroxidation). [10,11]

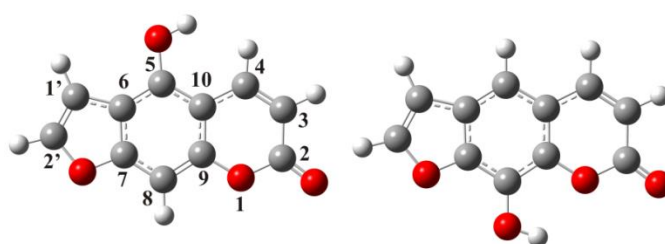


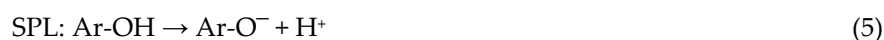
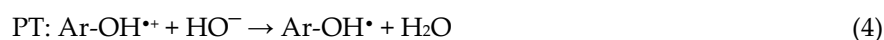
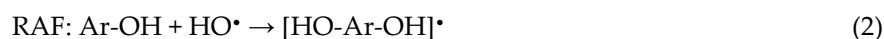
Figure 1. The optimized geometries of **BER** (left) and **XAN** (right) in benzene with atomic numbering.

This study includes the examination of the antioxidant capacity of thermodynamically favorable pathways from the kinetic aspect. Besides the standard mechanisms for investigating antioxidant activity: hydrogen atom transfer (HAT), single-electron transfer–proton transfer (SET-PT), sequential proton loss electron transfer (SPLET), the radical adduct formation (RAF) mechanism was also investigated. The investigation was performed in a non-polar environment, and for that purpose as solvent is used benzene. Examining and understanding the mechanisms of antiradical action in a nonpolar environment is of great importance in preventing lipid peroxidation. Preventing the effects of ROS on polyunsaturated fatty acids in the cell membrane contributes to maintaining normal cell functionality and permeability. The research was performed using the *Quantum Mechanics-based test for Overall free Radical Scavenging Activity* (QM-ORSA) protocol [12]. The obtained results were compared with the available literature data for Trolox (6-hydroxy-2,5,7,8-tetramethylchroman-2-carboxylic acid) through the value of *relative antioxidant capacity* (r^T).

2. Materials and Methods

All quantum chemical calculations were performed using the *Gaussian 09* software package. [13]. The M06-2X/6-311++(d,p) theoretical model was used to optimize the geometry and calculate the harmonic vibration frequencies of the investigated compounds. In addition to the structure and nature of ROS, the antioxidant activity of the compounds was found to be influenced by the microenvironment of the reaction medium. For this reason, benzene was chosen to mimic the nonpolar environment that is present in the cellular structure. The CPCM solvation model was applied to optimize structures in benzene, without any geometric constraints. The first step of investigating the inactivation of HO• radicals involves testing the thermodynamic parameters using the following equations:





where Ar-OH, Ar-O \cdot , (HO-Ar-OH) \cdot , Ar-OH $\bullet+$, and Ar-O $^-$ denote antioxidant, its radical, radical adduct, radical cation, and anion, respectively.

For the previously determined thermodynamic favorable reaction pathways (HAT mechanism) as well as for the RAF mechanism in this study, the corresponding kinetic parameters were calculated. [9]. All examined reactions are bimolecular. In the case where the structure of transition state (TS) exists between the reactants and products (HAT and RAF), the rate constant was calculated using the conventional transition state theory (TST) or Eyring equation [14]:

$$k_{\text{TST}} = \frac{k_{\text{B}}T}{h} \exp\left(\frac{-\Delta G_a^\ddagger}{RT}\right) \quad (7)$$

where k_{B} and h stand for the Boltzmann and Planck constants, T is temperature, R is gas constant (8.314 J mol $^{-1}$ K $^{-1}$) and ΔG_a^\ddagger is Gibbs free energy of activation.

In the case of the HAT and RAF mechanisms, it is necessary to include the values of the degeneracy of the reaction path, σ , and the transmission coefficient, γ (T) in the previous equation, implying that the Eyring equation transforms into:

$$k_{\text{ZCT-0}} = \sigma\gamma(T) \frac{k_{\text{B}}T}{h} \exp\left(\frac{-\Delta G_a^\ddagger}{RT}\right) \quad (8)$$

TheRate program was used to, determine rate constants [15]. The rate constants were calculated for 1 M standard state using the Eckart method, also known as ZCT-0 [16].

As in experimental research, theoretical research is also possible to determine the relative antioxidant capacity (r^T), relative to trolox (**Tx**) as the reference antioxidant. The ratio between the overall rate constant of examined antioxidant, k_{overall} , and the overall rate constant of **Tx**, $k_{\text{overall}}^{\text{Tx}}$ (under the same conditions), quantifies antioxidant capacity of the antioxidant compared to **Tx** [12]:

$$r^T = \frac{k_{\text{overall}}}{k_{\text{overall}}^{\text{Tx}}} \quad (9)$$

Also, based on the calculated k_{overall} values, it is possible to determine the relative amount of products (%), i.e. branching ratios (Γ_i), as well as to evaluate which of the mechanistic pathways, i , is dominant [12]:

$$\Gamma_i = \frac{k_i}{k_{\text{overall}}} \times 100 \quad (10)$$

3. Results and Discussion

3.1. Thermodynamic parameters

In the first phase of this research thermodynamically favorable reaction pathways were determined. The results of thermodynamic parameters in benzene from the previous study indicate that **BER** (-162 kJ mol $^{-1}$) and **XAN** (-137 kJ mol $^{-1}$) inactivate the HO \cdot radical via the HAT mechanism. The non-polarity of the medium limits the electronic transitions, which is why both compounds do not express their antioxidant capacity via the SET-PT and SPLET mechanisms. Additionally, the

thermodynamic parameters for the RAF mechanism were estimated. The possible reaction pathways as well as results of the thermodynamic parameters for the RAF mechanism are given in Figure 2 and Table 1.

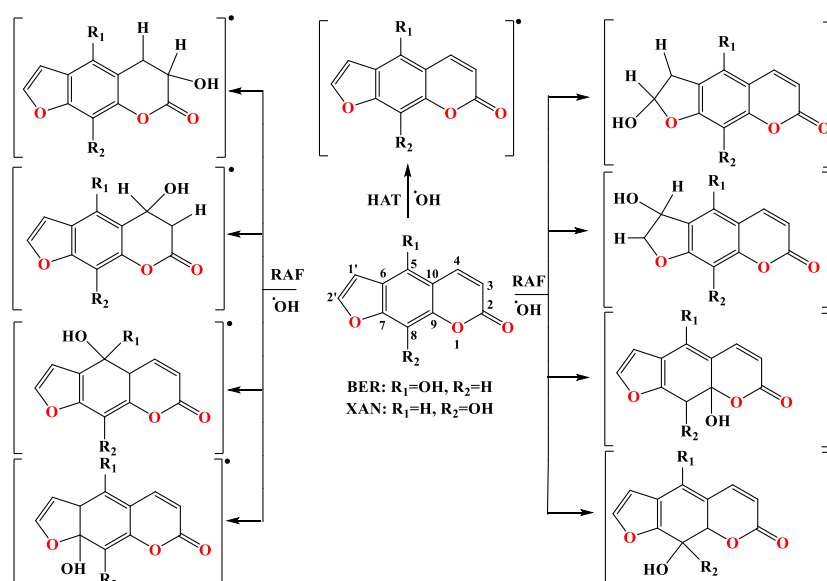


Figure 2. The scheme of the thermodynamic possible mechanism of inactivation HO• radical in benzene.

The endergonic values obtained for positions C-6 and C-10 for both compounds exclude these positions in the interpretation of antioxidant capacity from a kinetic aspect. Distinctly exergonic values are observed in the C-2' positions of the furan ring of investigated compounds. Additionally, the presence of a negatively concentrated charge on the C-3 atom of **BER** (-0.316 *e*) and **XAN** (-0.321 *e*) makes these positions attractive to the attack of electrophilic HO• radicals. This is reflected in pronouncedly negative Δ_rG values for these positions.

Table 1. Reaction free energies, Δ_rG (kJ mol⁻¹) produced at the M06-2X/6-311++G(d,p) level of theory in combination with the CPCM solvation model.

Position	HAT ^a	SET-PT ^a	SPLET ^a
BER	-162	334	-495
XAN	-137	340	-478
Position	BER	XAN	
C-3	-88	-79	
C-4	-75	-59	
C-5	-85	-82	
C-6	20	34	
C-7	-27	-32	
C-8	-42	-65	
C-9	-55	-60	
C-10	4	17	
C-1'	-52	-43	
C-2'	-120	-109	

^aThe presented values were taken from Ref. [9].

3.2. Kinetic parameters

The estimated values of the kinetic parameters for HAT and RAF mechanisms are given in Table 2. The optimized geometries of the transition states are presented in Figures 3 and 4.

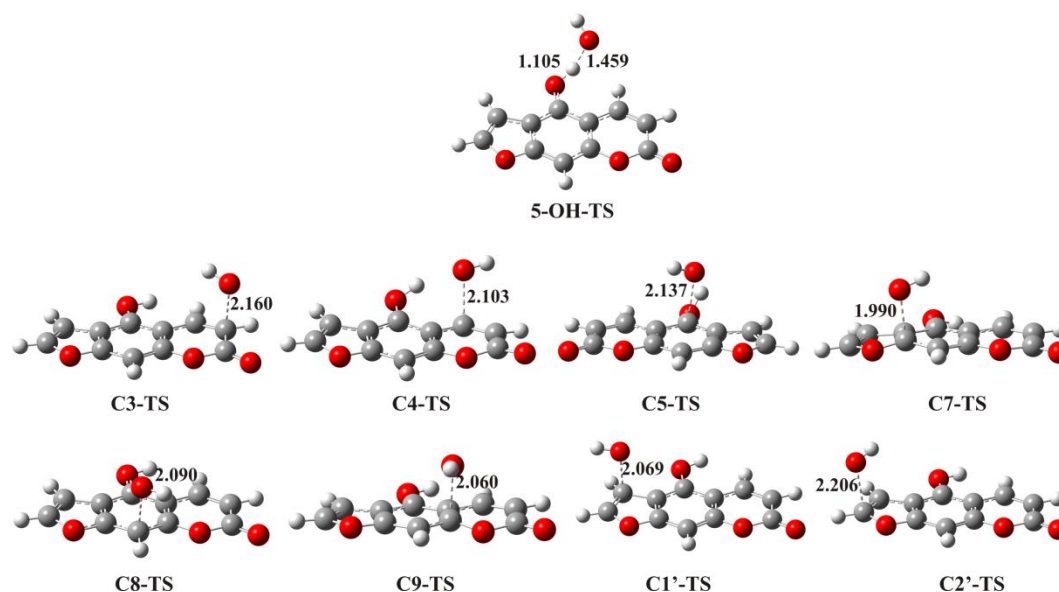


Figure 3. Optimized geometries of transition states for HAT and RAF pathways of **BER** in benzene with characteristic distance (Å) calculated at the M06-2X/6-311++G(d,p) level of theory in combination with the CPCM solvation model.

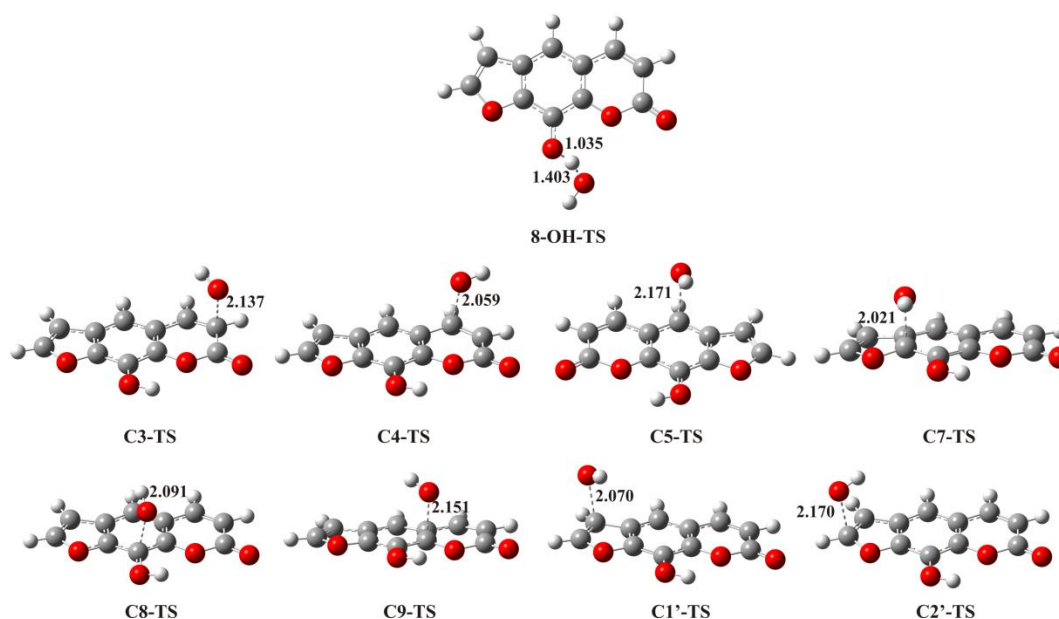


Figure 4. Optimized geometries of transition states for HAT and RAF pathways of **XAN** in benzene with characteristic distance (Å) calculated at the M06-2X/6-311++G(d,p) level of theory in combination with the CPCM solvation model.

In the HAT mechanism of **BER**, a deviation is observed in the values of the velocity constants estimated by the TST and Eckart method. Also, the opposite of the constants is observed in the thermodynamically most favorable C-2 'positions for the RAF mechanism. This indicates that the TST method is not suitable for assessing the rates of these reactions at room temperature. The fact that both mechanisms involve light particles capable of penetrating activation barriers, the

differences between the calculated constants can be attributed to the tunneling effect. Large values of the interatomic distance C-2'-OH in the geometries of transition states of the **BER** (2.206 Å) and **XAN** (2.170 Å) lead to the conclusion that these are early transition states. These reaction pathways are characterized by small values of activation energy, so by failing the TST theory it can be attributed to flat surfaces of potential energy.

Table 2. Activation energies ΔG_a^\ddagger (kJ mol⁻¹) and rate constants: k_{TST} (M⁻¹s⁻¹) and k_{ZCT_0} (M⁻¹s⁻¹) produced at the M06-2X/6-311++G(d,p) level of theory in combination with the CPCM solvation model.

Mechanism	BER			XAN		
HAT	ΔG_a	k_{TST}	k_{ZCT_0}	ΔG_a	k_{TST}	k_{ZCT_0}
		22	2.23x10 ¹⁰	2.14x10 ⁸	38	2.78x10 ⁷
RAF	ΔG_a	k_{TST}	k_{ZCT_0}	ΔG_a	k_{TST}	k_{ZCT_0}
C-3	30	7.05x10 ⁸	1.44x10 ⁸	33	2.11x10 ⁸	1.06x10 ⁸
C-4	37	4.15x10 ⁷	4.37x10 ⁷	45	2.17x10 ⁶	3.02x10 ⁶
C-5	25	5.52x10 ⁹	1.21x10 ⁸	28	2.01x10 ⁹	1.28x10 ⁸
C-7	55	2.91x10 ⁴	4.34x10 ⁴	45	1.81x10 ⁶	2.53x10 ⁶
C-8	34	1.80x10 ⁸	9.41x10 ⁷	35	1.15x10 ⁸	7.46x10 ⁷
C-9	42	6.47x10 ⁶	8.93x10 ⁶	29	1.07x10 ⁹	5.68x10 ⁷
C-1'	37	4.20x10 ⁷	5.02x10 ⁷	38	3.46x10 ⁷	4.22x10 ⁷
C-2'	23	1.51x10 ¹⁰	1.56x10 ⁸	28	2.10x10 ⁹	1.05x10 ⁸

Figure 5 shows the graphs of the dependence of the change in the rate constant ($\ln k$) on the temperature ($1/T$). In the 5-OH position of **BER** and C-2' positions of **BER** and **XAN**, it is observed that the k_{TST} constant decreases with increasing temperature and that the values are significantly less than k_{ZCT_0} . On the other hand, in 8-OH of **XAN** k_{TST} increases with increasing temperature while all values are higher than k_{ZCT_0} . In all presented cases, the constants calculated by the Eckart method are overestimated at low temperatures.

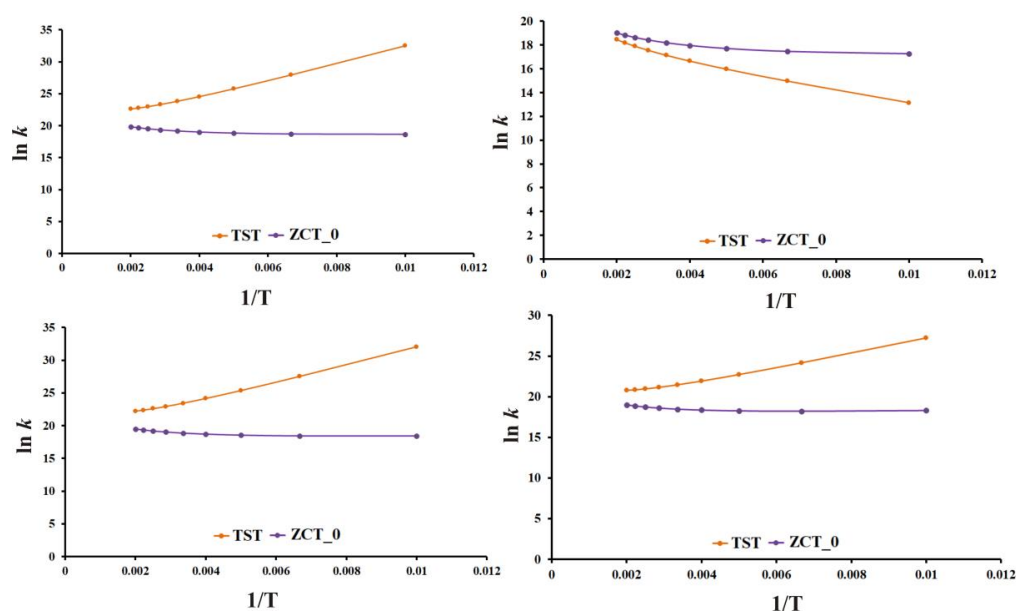


Figure 5. The plots of dependence k_{TST} (M⁻¹s⁻¹) and k_{ZCT_0} (M⁻¹s⁻¹) on $1/T$ in HAT (**BER** (a) and **XAN** (b)) and RAF (C-2' positions of **BER** (c) and **XAN** (d)) pathways.

3.3. Relative antioxidant capacity

A comprehensive examination of antioxidant activity from the kinetic aspect enables the assessment of relative antioxidant capacity (r^T) concerning the reference standard. **Tx** was chosen as the reference compound. The application of the same theoretical model and methodology, within the available literature data, justifies the choice of this standard. The value of the estimated overall rate constant for **Tx** in benzene, $k_{overall}^{Tx}$ is $1.31 \times 10^8 \text{ M}^{-1} \text{ s}^{-1}$ [17]. The sum of the rate constants for all favorable reaction pathways is the overall rate constant of the investigated compounds ($k_{overall}^{BER}$ and $k_{overall}^{XAN}$) whose values are given in Table 3.

Table 3. The $k_{overall}$ ($\text{M}^{-1}\text{s}^{-1}$), antioxidant capacity (r^T) and branching ratios (Γ_i , %) for all favorable mechanistic pathways.

Mechanism	Position	BER (%)	XAN (%)
HAT	OH	25.72	13.36
RAF	C-3	17.31	17.72
	C-4	5.25	0.50
	C-5	14.54	21.40
	C-7	0.01	0.42
	C-8	11.31	12.47
	C-9	1.07	9.50
	C-1'	6.03	7.06
	C-2'	18.75	17.56
$k_{overall}$		8.32×10^8	5.98×10^8
r^T		6.35	4.57

Ineffective primary antioxidants are considered to be compounded with total values $< 1.18 \times 10^3 \text{ M}^{-1} \text{ s}^{-1}$ [12]. As the values of $k_{overall}^{BER}$ and $k_{overall}^{XAN}$ exceed this value, they can be declared effective primary antioxidants. The relationship between $k_{overall}^{BER}$ of investigated antioxidants and **Tx** indicates greater or lesser antioxidant activity relative to **Tx**. The obtained values of **BER** and **XAN** with HO^\bullet radical in benzene indicate that both compounds are more reactive than **Tx**. The **BER** compound shows a more significant ability to inactivate HO^\bullet radicals compared to **XAN**. Based on the assessment of the relative amount of products, for **BER**, it is concluded that the formation of radical at 5-OH position (25.72 %) and radical adducts at positions: C-3 (17.31 %), C-5 (14.54 %), C-8 (11.31 %), and C-2' (18.75 %) most significantly. Similarly, in the case of **XAN**, the largest share of educated adducts is in positions C-3 (17.72 %), C-5 (21.40 %), C-8 (12.47 %), C-9 (9.50 %) and C-2' (17.56 %) as well as at 8-OH (13.36 %) position. Consequently, RAF is the dominant mechanism involved in the HO^\bullet scavenging activity of **BER** and **XAN**.

4. Conclusion

Within this study, the influence of the nonpolar medium in the mechanism of inactivation of HO^\bullet was investigated for **BER** and **XAN**. Estimated thermodynamic parameters indicate that both compounds exhibit their antioxidant activity through HAT and RAF mechanisms. Based on the estimated kinetic parameters, it can be concluded that the TST method is not suitable for the calculation of the rate constants for reactions that take through the geometry of the early transition states. Estimated values of relative antioxidant capacity indicate a better ability **BER** and **XAN** on HO^\bullet radical scavenging than **Tx**. In addition, **BER** possesses a better antioxidant ability than **XAN**.

Based on the relative amount of product, it can be concluded that for both compounds the RAF mechanism is dominant.

Author Contributions: For research articles with several authors, a short paragraph specifying their individual contributions must be provided. The following statements should be used “Conceptualization, Žiko Milanović, and Zoran Marković; methodology, Žiko Milanović; software, Marko Antonijević; validation, Jelena Đorović Jovanović, Dejan Milenković, and Edina Avdović; formal analysis, Dejan Milenković; investigation, Žiko Milanović; resources, Zoran Marković; data curation, Jelena Đorović Jovanović; writing—original draft preparation, Edina Avdović; writing—review and editing, Zoran Marković; visualization, Edina Avdović; supervision, Zoran Marković; project administration, Zoran Marković; funding acquisition, Zoran Marković. All authors have read and agreed to the published version of the manuscript.

Funding: This research was funded by the Serbian Ministry of Education, Science, and Technological Development (Agreement Nos 451-03-68/2020-14/200122 and 451-03-68/2020-14/200378).

Conflicts of Interest: The authors declare no conflict of interest.

References:

1. Apel, K.; Hirt, H. Reactive oxygen species: metabolism, oxidative stress, and signal transduction. *Annu. Rev. Plant Biol.*, **2004**, *55*, 373-399.
2. Bian, S.; Jiang, Y. Reactive oxygen species, antioxidant enzyme activities and gene expression patterns in leaves and roots of Kentucky bluegrass in response to drought stress and recovery. *Sci. Hortic.*, **2009**, *120* (2), 264-270.
3. Turrens J. F. Mitochondrial formation of reactive oxygen species. *J. Physiol.*, **2003**, *552*(2), 335-344.
4. Sunil Paul, M. M.; Aravind, Usha K.; Pramod, G.; Aravindakumar, C.T. Oxidative degradation of fensulfothion by hydroxyl radical in aqueous medium. *Chemosphere*, **2013**, *91* (3), 295–301.
5. Reiter, R. J.; Melchiorri, D.; Sewerynek, E. A review of the evidence supporting melatonin's role as an antioxidant. *J. Pineal Res.*, **1995**, *18* (1), 1–11.
6. Pathak, M. A.; Daniels, Jr F.; Fitzpatrick, T. B. The presently known distribution of furocoumarins (psoralens) in plants. *J. Invest. Dermatol.*, **1962**, *39*(3), 225-239.
7. Fylaktakidou, K. C.; Hadjipavlou-Litina, D. J.; Litinas, K. E.; Nicolaidis, D. N. Natural and synthetic coumarin derivatives with anti-inflammatory/antioxidant activities. *Curr. Pharm. Des.*, **2004**, *10* (30), 3813-3833.
8. Camm, E. L.; Wat, C. K.; Towers, G. H. N. An assessment of the roles of furanocoumarins in *Heracleum lanatum*. *Can. J. Bot.*, **1976**, *54* (22), 2562–2566.
9. Milanović, Ž.; Antonijević, M.; Đorović, J.; Milenković, D. Comparative Antiradical Activity and Molecular Docking Study of Bergaptol and Xanthotoxol, *J. S. C. C. M.*, **2020**, *Special issue 2020*, 71-84.
10. Devienne, K. F.; Cálgaro-Helena, A. F.; Dorta, D. J.; Prado I. M.; Raddi M. S. G.; Vilegas, W., Curti, C. Antioxidant activity of isocoumarins isolated from *Paepalanthus bromelioides* on mitochondria. *Phytochemistry*, **2007**, *68*(7), 1075-1080.
11. Girenavar, B.; Jayaprakasha, G. K.; Jadegoud, Y.; Gowda, G. N.; Patil B. S. Radical scavenging and cytochrome P450 3A4 inhibitory activity of bergaptol and geranylcoumarin from grapefruit. *Bioorg. Med. Chem.*, **2007**, *15*(11), 3684-3691.
12. Galano, A.; Alvarez-Idaboy, J. R. A computational methodology for accurate predictions of rate constants in solution: application to the assessment of primary antioxidant activity. *J. Comput. Chem.*, **2013**, *34*, 2430–2445.
13. Frisch, M. J.; Trucks, G. W.; Schlegel, H.B.; Scuseria, G. W.; Robb, M. A.; Cheeseman, J. R.; Scalmani, G.; Barone, V.; Mennucci, B.; Petersson, G. A.; Nakatsuji, H.; Caricato, M.; Li, X.; Hratchian, H. P.; Izmaylov, A. F.; Bloino, J.; Zheng, G.; Sonnenberg, J. L.; Hada, M.; Ehara, M.; Toyota, K.; Fukuda, R.; Hasegawa, J.; Ishida, M.; Nakajima, T.; Honda, Y.; Kitao, O.; Nakai, H.; Vreven, T.; Montgomery, J. A.; Peralta, J. E.; Ogliaro, F.; Bearpark, M.; Heyd, J. J.; Brothers, E.; Kudin, K. N.; Staroverov, V. N.;

- Kobayashi, R.; Normand J.; Raghavachari, K.; Rendell, A.; Burant, J. C.; Iyengar, S. S.; Tomasi, J.; Cossi, M.; Rega, N.; Millam, J. M.; Klene, M.; Knox, J. E.; Cross, J. B.; Bakken, V.; Adamo, C.; Jaramillo, J.; Gomperts, R.; Stratmann, R. E.; Yazyev, O.; Austin, A. J.; Cammi, R.; Pomelli, C.; Ochterski, J. W.; Martin, R. L.; Morokuma, K.; Zakrzewski, V. G.; Voth, G. A.; Salvador, P.; Dannenberg, J. J.; Dapprich, S.; Daniels, A. D.; Farkas, Ö.; Foresman, J. B.; Ortiz, J. V.; Cioslowski, J.; Fox, D. J. **2009**, *Gaussian 09*.
14. Eyring, H. The activated complex in chemical reactions. *J. Chem. Phys.*, **1935**, *3*, 107-115.
15. Duncan, W. T.; Bell, R. L.; Truong, T. N. TheRate: Program for ab initio direct dynamics calculations of thermal and vibrational-state-selected rate constants. *J. Comput. Chem.*, **1998**, *19*, 1039–1052.
16. Eckart, C. The penetration of a potential barrier by electrons. *Phys. Rev.*, **1930**, *35*, 1303–1309.
17. Tošović, J.; Marković, S. Reactivity of Chlorogenic Acid toward Hydroxyl and Methyl Peroxy Radicals Relative to Trolox in Nonpolar Media. *Theor. Chem. Acc.*, **2018**, *137*, 76.

Publisher's Note: MDPI stays neutral with regard to jurisdictional claims in published maps and institutional affiliations.



© 2020 by the authors. Submitted for possible open access publication under the terms and conditions of the Creative Commons Attribution (CC BY) license (<http://creativecommons.org/licenses/by/4.0/>).